Avalanche Breakdown in Gallium Arsenide *p-n* Junctions

R. A. LOGAN, A. G. CHYNOWETH, AND B. G. COHEN
Bell Telephone Laboratories, Murray Hill, New Jersey

(Received June 18, 1962)

Charge multiplication and avalanche breakdown have been studied in relatively narrow diffused *p-n* junctions in GaAs. For these studies both junctions with and without microplasma effects were available. From the charge multiplication studies in microplasma-free junctions, the ionization rate, α, has been determined as a function of the field, $\mathcal{E}$. These results are unusual in that they give a decidedly better fit to Wolff's theory than to Shockley's; this is found to be consistent with the criterion, $e\mathcal{E}\lambda >$ (optical-phonon energy), discussed in a more recent theory due to Baraff which combines the approaches of both Wolff and Shockley. From detailed comparisons with Baraff's theory, the mean free path, λ, for the hot carriers between collisions involving optical phonon emission is 15 ± 2 Å and the threshold energy for pair production is 1.7 ± 0.3 eV.

Strong correlations were found between the quality of the breakdown (i.e., formation or absence of microplasmas) and the quality of the substrate crystal. Those junctions that exhibited microplasma noise and several multiplication peaks also had soft reverse characteristics, whereas the junctions that appeared to be free from microplasmas had hard breakdown characteristics. With the soft junctions, quantitative comparisons were made between the dark current and the number of microplasmas.

INTRODUCTION

THE abrupt reverse-bias breakdown of *p-n* junctions into a high-current condition ascribed to avalanche multiplication has been intensively studied in silicon and germanium. The extension of the study of this phenomenon to other semiconductors has awaited the development of the technology necessary to fabricate junctions of suitable geometry and impurity doping. Recently, avalanche breakdown effects have been reported in GaP junctions,[1] and the present work describes studies of reverse-bias breakdown in GaAs junctions. While straightforward avalanche multiplication causes the breakdown in junctions made with some GaAs crystals, in others, a high-current condition is observed at junction fields which are low enough that ordinary avalanche multiplication effects are small. In these junctions current flow is almost entirely by microplasma formation and this is accompanied by the familiar microplasma noise.

In this paper, measurements are described on the reverse bias dependence of (i) the dark current, (ii) the photo current, and (iii) the capacitance. Also, in those junctions that exhibit microplasma effects, the number of microplasmas is correlated with the diode current and voltage. For junctions which break down without evidence of microplasma formation, the bias dependence of the capacitance and photocurrent are used to determine the ionization rate, α, as a function of field, $\mathcal{E}$.

It will be shown that the observed dependence of α upon $\mathcal{E}$ is incompatible with Shockley's theory[2] for these junctions, but instead, it may be interpreted in terms of Wolff's theory[3] or the more recent theory of Baraff.[4]

Finally, since the manner of breakdown appears to depend markedly upon the crystal properties, these are discussed, although the detailed causes of microplasma formation are not known at present.

EXPERIMENTAL AND RESULTS

Fabrication of the Junctions

The junctions were made by diffusing Cd or Zn in a closed quartz system under an inert atmosphere into *n*-type wafers of GaAs of resistivity ranging from 0.001 or 0.02 Ω cm. Some of the properties of the *n*-type crystals will be listed in a later section where a correlation with the multiplication results will be presented. Representative diffusion cycles were 800°C for 30 min for Zn and 900°C for 125 h for Cd. Typical values of the *p*-type layer thickness and sheet resistivity were 0.3 mil, 5 Ω/sq and 0.1 mil, 100 Ω/sq for Zn and Cd diffusions, respectively. Contact to the *n*-type GaAs was achieved using a technique developed by Sharpless.[5] The steps in this process are: (1) evaporation of Sn onto the sample while the latter is heated to 200°C, (2) electroplate with Ni, (3) sinter at 600°C for 10 min, (4) electroplate with Ni, and, finally, (5) electroplate with Au. The *n*-type side was then soldered to a conventional diode header. The diffused layer was electroplated with Ni and then gold. Contact to this layer was achieved by pressing a point against the plated surface. The junction was delineated using conventional waxing and etching techniques and was typically 2–4 mil in diam. In those junctions used for photo-current studies, the electroplated layer covered approximately one-half of the diffused layer surface.

Current Voltage Characteristics

The diodes used in this study were made from two different crystals and on the basis of a survey of hundreds of diodes, they could be sharply divided into two classes, namely, those with and those without microplasma effects; the microplasma effects show up

[1] R. A. Logan and A. G. Chynoweth, J. Appl. Phys. **33**, 1649 (1962).
[2] W. Shockley, Czech. J. Phys. **B11**, 81 (1961) and Solid-State Electron. **2**, 35 (1961).
[3] P. A. Wolff, Phys. Rev. **95**, 1415 (1954).
[4] G. A. Baraff, preceding paper [Phys. Rev. **128**, 2507 (1962)].
[5] W. M. Sharpless, Bell System Tech. J. **38**, 259 (1959).

as both the characteristic microplasma noise[6,7] and as singularities in the multiplication characteristics.[8,9] In the following, junction A is representative of junctions which do not exhibit detectable microplasma generation, while junctions B and C are representative of those that do. Semilogarithmic plots of the reverse current (I) vs voltage (V) are shown in Fig. 1 at 78, 196, and 300°K. It is clear that while breakdown voltages are well defined for the two junctions they differ in two distinct aspects: In junction B, the abrupt increase in current correlates with the formation of the first microplasma which carries the current up to above 10 μA. Upon the generation of further microplasmas, the current increases exponentially with bias with the empirical form

$$I = I_0 \exp(\mu V),$$

with $\mu = 1.0$ V^{-1}. The coefficient μ increases with decreasing temperature. Hence, although there is a well-defined voltage, V_B, at the *onset* of breakdown, the bias increases appreciably as the current increases, i.e., the breakdown is relatively "soft." In junction A, on the other hand, there is no evidence of a soft breakdown. A second distinction between the two junctions is the rate of the linear decrease of V_B with temperature, the rate being much greater for junction B. The coefficient

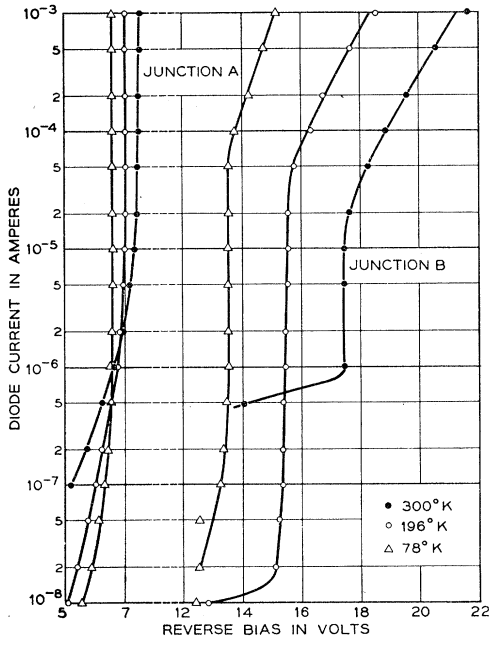

FIG. 1. Semilogarithmic plot of the reverse current vs the applied bias at three different ambient temperatures for junction A (with breakdown by avalanche multiplication) and for junction B (with breakdown by microplasma generation).

[6] K. G. McKay, Phys. Rev. **94**, 877 (1954).
[7] A. G. Chynoweth and K. G. McKay, J. Appl. Phys. **30**, 1811 (1959).
[8] R. L. Batdorf, A. G. Chynoweth, G. C. Dacey, and P. W. Foy, J. Appl. Phys. **31**, 1153 (1960).
[9] M. Kikuchi, J. Phys. Soc. Japan **15**, 835 (1960) and M. Kikuchi and K. Tachikawa, *ibid.* **15**, 1822 (1960).

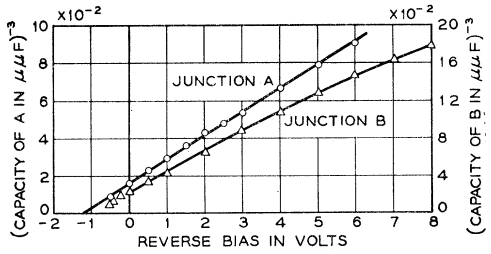

FIG. 2. Plots of (capacitance)$^{-3}$ vs applied bias for junctions A and B.

$\beta = V_B^{-1}(300°\text{K})\partial V_B/\partial T$ is 5.3×10^{-4}(°K)$^{-1}$ for junction A and 1.2×10^{-3}(°K)$^{-1}$ for junction B.

Semilogarithmic plots of the forward current vs bias were linear with slope $e/(nkT)$, with $n = 1.3$ for junction A and $n = 2.2$ for junction B, where e is the electron charge, k is Boltzmann's constant, and T is the absolute temperature. These values of n are typical of the junctions studied and may be ascribed to nonlinear carrier recombination. Ohmic-series resistance effects were negligible for $I < 10^{-3}$ A.

Capacitance Data

The junction capacitance was measured as a function of bias to within about one volt of V_B. Typical plots of C^{-3} vs V are shown in Fig. 2 for junctions A and B. While it is evident that junction A accurately follows the cube law, as expected, junction B does not. This difference in capacitance behavior correlates strongly with the diffusant used to form the junction and not with the crystal properties. Junction A was formed by cadmium diffusion, while junction B was made using Zn as the diffusant. The breakdown properties of the junctions, on the other hand, correlate only with the crystal properties and are independent of the diffusant or diffusion heating cycle. While the reason for this capacitance anomaly is not understood in detail, it should be noted that while Cd diffuses substitutionally, Zn does not obey Fick's law. The impurity profile obtained with Zn might also be distorted by precipitation effects which may occur during the cooling cycle, aided by the relatively rapid diffusivity of Zn. Empirically, it was observed that the capacitance of zinc diffused junctions obeyed a power law between 2 and 3, the actual index varying from junction to junction. The built-in voltage for Zn diffused junctions ($\sim$1.0 V) was also lower than that in Cd junctions ($\sim$1.25 V). In view of the capacitance results, no attempt was made to interpret quantitatively the avalanche multiplication studies using Zn diffused junctions because of the uncertainties in the electric field distribution in these junctions.

Photocurrent vs Bias

Using both white and monochromatic light sources, the short-circuit photocurrent, I_p, generated at the junction was measured as a function of bias using

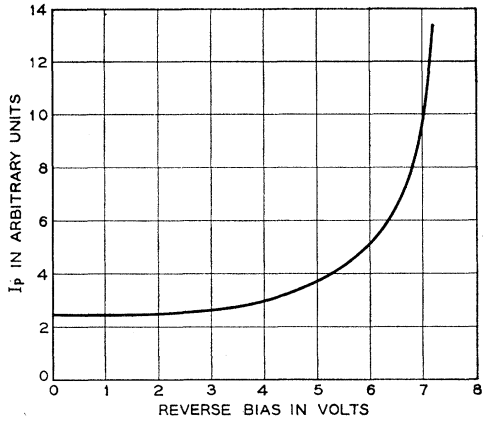

FIG. 3. The photocurrent plotted against the reverse bias for junction A. The slight increase in I_p up to $V=2.5$ V (which is obscured by the small dimensions of the figure) is ascribed to space-charge widening whereas at higher biases multiplication effects dominate.

equipment that has been described elsewhere.[10] The I_p-V curve for junction A is shown in Fig. 3. This curve was obtained with white light, but was in exact agreement with that obtained using monochromatic light of energy 1.6 eV where the absorption coefficient[11] is $\sim 10^4$ cm^{-1}. This result is taken as evidence that the junctions are spatially uniform since in the latter case, carriers are not generated under the contact to the junction. In addition, the I_p-V curve was independent of the intensity of the incident light indicating that field distortion due to injected carriers was of no significance. It is noted that the photocurrent increases slightly with bias before the more rapid increase associated with carrier multiplication. If this initial increase is ascribed to the reverse widening of the space-charge region,[1] then a plot of I_p vs W gives an intercept at $I_p=0$ of $L_D=3\times10^{-5}$ cm, the sum of the minority carrier diffusion lengths on either side of the junction. The junction width constant is 400 Å, a value not insignificant in comparison with L_D. While this aggregate length cannot be assigned to a specific lifetime, if one uses the known carrier mobilities in GaAs, this diffusion length would correspond to lifetimes of either $\sim 10^{-10}$ or $\sim 10^{-11}$ sec for holes and electrons, respectively, values not unreasonable for this material. It is also noted that the transit time for carriers across the junction ($\sim 10^{-12}$ sec) is small compared to the estimated lifetimes.

Having corrected for the small junction widening effect described above, the ionization rate, α, was computed as a function of the maximum electric field, $\mathcal{E}_m$ by assuming that α was the same for both electrons and holes and using the formula,[12]

$$1-1/M=\int_0^W \alpha(\mathcal{E})dx=0.4W\alpha(\mathcal{E}_m)$$

where W is the width obtained from the capacity measurements. The use of this formula in narrow junctions will ultimately fail as junction dimensions become comparable to distances characteristic of the ionization process. The exact calculation of α then becomes extremely complex. However similar studies[13] in silicon junctions show that experimentally the above formula is valid in junctions with $V_B\sim 6E_G$ (E_G is the energy gap), as is the case here. To test the predicted dependence of α upon $\mathcal{E}_m$, Fig. 4 shows for junction A a plot of $\log(\alpha\mathcal{E}_m^{-1})$ vs $\mathcal{E}_m^{-1}$ as required by Shockley's theory[2] and a plot of $\log\alpha$ vs E_m^{-2} as required by Wolff's theory.[3] A linear relationship would imply agreement with theory. The results unlike those for silicon,[14] are clearly in favor of Wolff's theory, and equally good verification was obtained in four separate experiments on two different junctions.

Microplasma Breakdown

In studies of the bias dependence of the short-circuit photocurrent, I_p, it was observed that in some junctions there occurred a series of sharp, isolated peaks in the photocurrent. As will be noted, the occurrence of each of these peaks could be correlated with a burst of

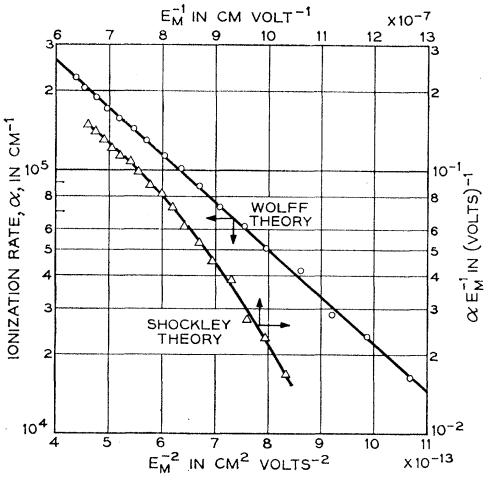

FIG. 4. Plots of the field dependence of the ionization rate in GaAs with the appropriate scales for each curve indicated by arrows.

[10] A. G. Chynoweth and K. G. McKay, Phys. Rev. **108**, 29 (1957).

[11] T. S. Moss and T. D. F. Hawkins, Infrared Phys. **1**, 111 (1961).

[12] The tacit assumption that the effective width remains a constant fraction of the total width for all applied biases can be shown to be true whenever $1-1/M$ is equal to $(V/V_B)^n$, where n is a constant, V_B is the breakdown voltage and M is the observed carrier multiplication at bias V. This empirical relationship is found to hold for most junctions, and in particular for junction A, $n=3.5$. With this relationship, the integrals in the usual expression for α can be evaluated analytically giving the effective width as 0.38 W. The appropriate integrations for step junctions are described by S. L. Miller, Phys. Rev. **99**, 1234 (1955). The authors are indebted to C. A. Lee for extending this work to the present studies.

[13] C. A. Lee, R. A. Logan, R. L. Batdorf, J. J. Kleimack, and W. Wiegmann (private communication).

[14] A. G. Chynoweth, Phys. Rev. **109**, 1537 (1958).

microplasma noise generated by the bistable current condition characteristic of microplasmas. At biases between the photocurrent peaks there was no detectable background multiplication. This microplasma formation was independent of the diffusion cycle and correlated only with the crystal used to fabricate the junction. The effect is demonstrated in Fig. 5, where plots are superimposed of the bias dependence of both I_p and the dark current for junction C, a junction similar to B.

It is evidence that beginning at a bias of 15.5 V, a microplasma forms as evidenced by a pronounced multiplication peak. The width of the peak is roughly comparable to the bias range over which microplasma instability is observed. As the bias is increased the phenomenon repeats, and, in regions where no new microplasmas form, I_p returns to values approximately equal to those in the premicroplasma region. Finally as the bias is further increased, microplasmas form at closer intervals in bias, and I_p increases in a discontinuous manner. Also shown in Fig. 5, is the bias

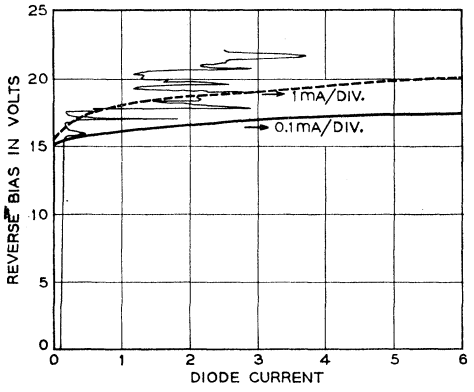

FIG. 5. The reverse bias dependence of the photocurrent and the dark current for junction C. Two plots of the dark current are given using different scales of 0.1 and 1.0 mA/div whereas the photocurrent is in arbitrary units.

dependence of the dark current, plotted on two different current scales of 0.1 mA/div and 1.0 mA/div. It is evident that the sudden dark current increase correlates with the formation of the first microplasma and that the dark current increases as further microplasmas are formed. From capacitance measurements, it is estimated that $\mathcal{E}_m$ is $\sim 10^6$ V/cm, at the formation of the first microplasma. As shown in Fig. 4, at this field one would expect avalanche multiplication effects to become important.

Multiplication peaks corresponding to individual microplasmas have been previously observed in silicon junctions where it was found that the relative magnitude of the peak decreased as the light intensity increased.[8] The multiplication peaks in the GaAs junctions show similar response to the light intensity.

By means of oscilloscope observations, the occurrence of microplasmas can be visually monitored by observing the voltage generated across a small resistance ($\sim$100 Ω) in series with the diode. As the microplasma is formed, noise indicative of the bistable current flow through it is observed on the oscilloscope. It was possible to correlate the formation of microplasma with the average dc diode current and the voltage across the diode.

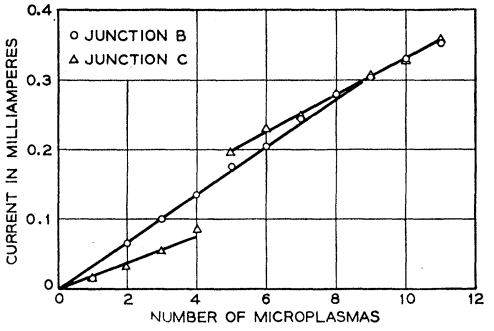

FIG. 6. The diode current plotted against the number of microplasmas for junctions B and C.

Representative plots of the number of microplasmas formed vs the diode current are shown in Fig. 6 for junctions B and C. The linear plot for junction B confirms that each microplasma carries, on the average, a current of approximately 33 μA. In junction C, on the other hand, four microplasmas form, each carrying about 20 μA of current, then a delay occurs before similar microplasmas are again generated. This effect is possibly caused by the growth of the four microplasmas in a sustained condition, as has been observed in silicon.[7]

The variation of junction voltage during the formation of microplasmas is shown in Fig. 7, where a semilogarithmic plot is made of the number of microplasmas against the applied bias. As already implied by the data presented in Figs. 1 and 6, the number of microplasmas increases exponentially with bias; similar behavior has

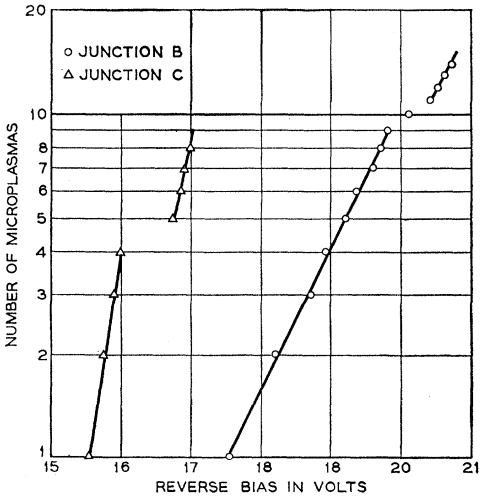

FIG. 7. The logarithm of the number of microplasmas plotted against the reverse bias for junctions B and C.

been observed in silicon also.[15] After the fourth microplasma in junction C, the bias increases from 16.0 to 16.75 V before further microplasmas are formed. Corroboration of these microplasma identifications comes from observation of the photocurrent in Fig. 5. It is seen that between the first two photocurrent peaks (which correspond to the two groups of four microplasmas of Fig. 7), I_p is at the premicroplasma value. The observation of microplasma formation by these techniques becomes limited at higher biases where the microplasmas are formed so close together that the bias resolution becomes uncertain.

For junctions such as B, where the number of microplasmas increases exponentially with bias and each carry approximately equal currents, I_0, then the expression for the bias dependence of current is

$$I = I_0 \exp \mu V,$$

where for junction B in Fig. 7, $\mu = 1.0\ \mathrm{V}^{-1}$ in agreement with the bias dependence of the current in the microplasma breakdown region shown in Fig. 1.

A visual study of these junctions was made for the light emission normally associated with microplasmas,[7,9] without success. This is not surprising over the main area of the junction because of the relatively large diffusion depth. However, it was regarded as surprising that no light was observed around the peripheries of the junctions.

As noted above, the occurrence or absence of microplasmas could be correlated with the parent crystals on which the junctions were fabricated. These crystals, which had slightly different resistivities, were grown by different methods. The low-resistivity wafers were obtained from a pulled crystal, doped with Sn, with a dislocation-etch-pit count typically $\sim 10^4\ \mathrm{cm}^{-2}$. The higher resistivity samples were obtained from a crystal grown without added dopant, by the Bridgman technique (zone leveled in a quartz boat). This crystal contained $\sim 10^6$ dislocations per cm^2, which is about 2 orders of magnitude larger than expected for the growth conditions. In addition, observation of crystal slices with an infrared microscope revealed unidentified precipitates, about 1 mil in diam and running in length approximately in the growth direction, nonuniformly distributed with local densities ranging from clear regions to as high as 500 cm^{-2}. Reverse bias breakdown in junctions made from the latter crystal was by microplasma formation. It is felt that the cause of microplasmas is more likely associated with the high dislocation density rather than the precipitates since microplasmas are observed in virtually every junction made from the crystal although the average distance between precipitates is large compared to the junction dimensions. Moreover, dislocations have been shown to be sites at which microplasmas may form in silicon. It should be emphasized that the correlation of microplasmas is with crystal perfection and not with the method of crystal growth, since equally perfect crystals may be grown by either technique.

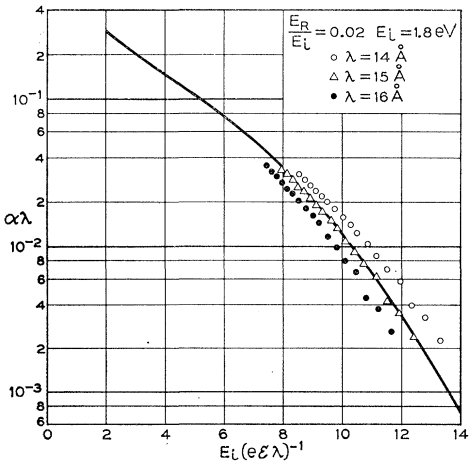

FIG. 8. Semilogarithmic plots of $\alpha\lambda$ vs $E_i(e\mathcal{E}\lambda)^{-1}$, using the parameters listed in the figure. The curve is from Baraff's theory for the case $E_R/E_i = 0.02$.

Discussion of Ionization Rate Results

Recently, Baraff[4] has given a more thorough theoretical treatment of the ionization rate problem than the earlier theories of Wolff[2] and Shockley.[3] In particular, Baraff shows that the two forms of the field dependence of α predicted by these older theories are two limiting cases of the more general treatment: Wolff's theory, which pertains to a swarm of electrons drifting across the junction with a particle velocity distribution maintained roughly spherically symmetrical by lattice scattering, is applicable at high fields, while Shockley's theory, which is basically concerned with those chance electrons which are accelerated into the high-energy tail of the velocity distribution without suffering energy-losing collisions, pertains to low fields. A very rough criterion for the cross over from the low- to the high-field condition is when

$$e\mathcal{E}\lambda \sim E_R,$$

where E_R is the energy of the optical phonon. (More detailed considerations actually suggest that the right-hand side of this criterion should be several times E_R, and as will be seen, this is certainly more in line with the experimental evidence.)

The end result of Baraff's theory is a set of universal curves of, essentially, $\log\alpha$ against $\mathcal{E}^{-1}$, involving three parameters: E_i, the ionization energy, E_R, and λ. For a given crystal, E_R is generally known, so that, in order to fit the experimental data to these curves, there are only two adjustable parameters. The results of fitting the experimental data to the theoretical curves are demonstrated in Figs. 8 and 9. With $E_R = 0.036$ eV for

[15] A. Goetzberger and C. Stephens, J. Appl. Phys. 32, 2646 (1961).

GaAs, the shape of theoretical curves is best fitted with $E_i=1.8$ eV and $\lambda=15$ Å as shown in Fig. 8 where, using the experimentally observed values of α and $\mathcal{E}_m$ and the above-selected parameters, log $\alpha\lambda$ is plotted against $E_i(e\mathcal{E}_m\lambda)^{-1}$. The curve drawn through the points is the appropriate theoretical curve of Baraff for $E_R/E_i=0.02$. The sensitivity of this agreement between theory and experiment to the choice of the parameter λ is also shown in Fig. 8 by making the same plots for values of $\lambda=14$ Å and 16 Å. It is evident that having selected a value of E_i to optimize the agreement in slope of the experimental and theoretical curves, the relative position of the two curves, is extremely sensitive to the choice of λ. Figure 9 demonstrates the effect of varying the parameter E_i. With $E_i=2.0$ eV and $\lambda=16.5$ Å, a best fit is obtained where the low field values of $\alpha\lambda$ lie below the appropriate theoretical curve ($E_R/E_i=0.018$); with E_i equal to the energy gap, 1.35 eV (the lower limit was assumed by Shockley in his analysis of the ionization rate in silicon) and $\lambda=12.5$ Å, the low field values of $\alpha\lambda$ lie above the theoretical curve ($E_R/E_i=0.027$). Hence, while it is possible to vary the parameter E_i to produce noticeably poorer fits to the theoretical curves, the departures are small for E_i in the range 1.35 to 2.0 eV. In this range of E_i, however, the parameter λ varied only from 12.5 to 16.5 Å. It is concluded, therefore, that there is good agreement with theory and experiment for $\lambda=15\pm2$ Å and $E_i=1.7\pm0.3$ eV.

With this value of λ, $e\mathcal{E}\lambda/E_R$ varies from 3.3 to 6.5 in the GaAs diodes in the range of electric field studied. It would therefore be expected that Wolff's theory rather than Shockley's would describe the dependence of α upon $\mathcal{E}$, over the entire range of $\mathcal{E}$, as has indeed been found. In silicon, on the other hand, the published data apply to an electric field range of 2–5×10^5 V cm^{-1} so that with $E_R=0.063$ eV and using $\lambda=50$ Å as determined by Shockley's theory, $e\mathcal{E}\lambda/E_R$ varies from 1.6 to 4.3, indicating the compatibility of the silicon results with Shockley's theory if Baraff's criterion is $e\mathcal{E}\lambda/E_R\sim3$ to 4.

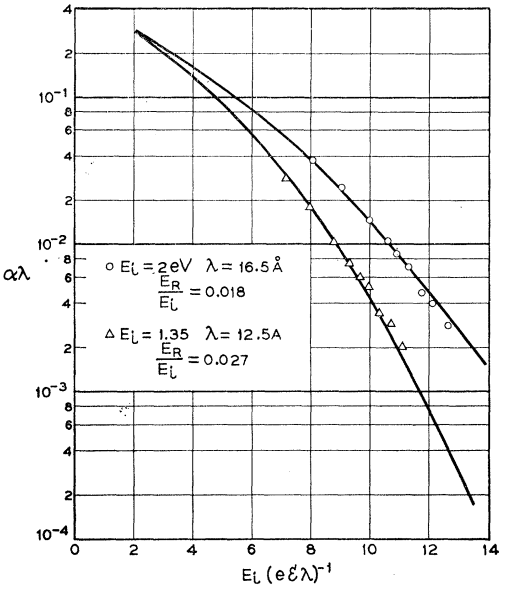

FIG. 9. Semilogarithmic plots of $\alpha\lambda$ vs $E_i(e\mathcal{E}\lambda)^{-1}$, using the parameters listed in the figure. The curves drawn are from Baraff's theory.

The authors are greatly indebted to G. A. Baraff for many valuable discussions, and to C. E. Youngdahl and A. R. Tretola for technical assistance.